Electronic dephasing of molecules in solution measured by nonlinear spectral inteferometry

Arkaprabha Konar[a], Vadim V. Lozovoy[a], Marcos Dantus[a,b,*]

[a] *Department of Chemistry, Michigan State University, East Lansing, Michigan 48824, United States*
[b] *Department of Physics and Astronomy, Michigan State University, East Lansing, Michigan 48824, United States*

[*] *Author for correspondence: Marcos Dantus, email: dantus@msu.edu*
Received 08 Jan 2014; Accepted 07 Feb 2014; Available Online 07 Feb 2014

Abstract

The dephasing time for the initial electronic coherence between the ground and excited states is significant because during this time quantum-mechanical phase can be expected to play a role in molecular processes. Dephasing measurements are particularly important for molecules in condensed phase where inhomogeneous broadening, changes in dipole, and solvent reorientation, complicate the observables. Here, phase-locked femtosecond pulse pairs are used to measure the coherent third-order response from IR144 and IR125 and the measurements are compared with simultaneous fluorescence measurements. For long time delays, out-of-phase oscillations for stimulated emission, that persist for approximately 130 fs or 180 fs for IR144 or IR125, respectively, are observed. We use phenomenological modeling to fit the oscillations and extract relevant parameters.

Keywords: Solvation dynamics; Decoherence; Pulse shaping

1. Introduction

Preparation and probing of coherent superposition of quantum states leading to quantum coherence in condensed phase systems has been the topic of intense research for over a decade. The solvent environment complicates these measurements through inhomogeneous broadening, changes in polarity, and by greatly increasing the number of degrees of freedom; making condensed phase molecules some of the most interesting and least understood quantum systems. Understanding the role of electronic coherence in photosynthetic pigment protein complexes is central to elucidating the mechanism of energy transfer therein [1-3]. Hierarchies of energy relaxation and energy dependent correlation have been found to result in non-exponential dephasing, leading to longer than expected coherence time, when compared to density of states arguments [4]. Nonlinear optical spectroscopy methods, such as photon echo and 2D electronic spectroscopy measurements, are particularly suitable for measuring electronic coherence [5, 6]. However, the future implementation of such coherent spectroscopic methods, requiring phase matching conditions, under single molecule conditions may be impossible. Therefore, inspired by single-beam coherent spectroscopic methods [7-10], we are exploring the use of a single shaped laser pulse to explore coherence [11-14]. Here, we present an approach that is directly sensitive to electronic coherence dephasing.

The approach followed in this study is a nonlinear variation of spectral interferometry. We stress the nonlinear nature of our approach because in a linear measurement, when the signal is proportional to the population of the excited state, the measurement is equivalent to the Fourier transform of the absorption spectrum of the quantum system multiplied by the spectrum of the two pulses sequence [15-17]. However, it has been noted that one is able to use spectral interferometry under nonlinear conditions in order to measure the system dynamics of interest [18-20]. Here we exploit this observation, measuring the third-order coherent emission of molecules in condensed phase, to obtain the desired electronic dephasing information. More complex collinear measurements using pulse shapers have been used to study rubidium atom vapors [21], one and two photon 2D electronic spectra of Coumarin 102 [10], and conformations of self-assembled dimers in liposomes [22] while collecting the fluorescence spectra at right angles.

Measurements are performed on IR144 and IR125 in solution, which have been model compounds for studying solvation because of their high absorption cross section near 800 nm and their considerable solvent-dependent Stokes shift. The solvatochromatic behavior of these cyanine dyes has been extensively investigated using pump-probe [23] and four-wave mixing [24] experiments performed by Jonas and coworkers. IR144 has been found to diphase faster presumably because of the piperazine moiety which is lacking in IR125. Coherent wave-packet motion of IR 144 on the ground and excited state surfaces has been studied using time resolved dynamic absorption spectroscopy [25] and by coherence period resolved transient grating [26]. Our group has recently put forward a model for explaining the early optical response and complementary behavior between fluorescence and stimulated emission for IR144, following studies based on phase-locked non-interfering pulses [13] and chirped femtosecond pulses [12].

2. Experimental Details

A. Laser system

The femtosecond laser system used for this study (Figure 1) consists of a regeneratively amplified Ti:Sapphire laser (Spitfire, Spectra-Physics) seeded by a Ti:Sapphire oscillator (KM Labs). The output from the amplifier at 1 kHz centered at 800 nm having a bandwidth of 26 nm (FWHM) is

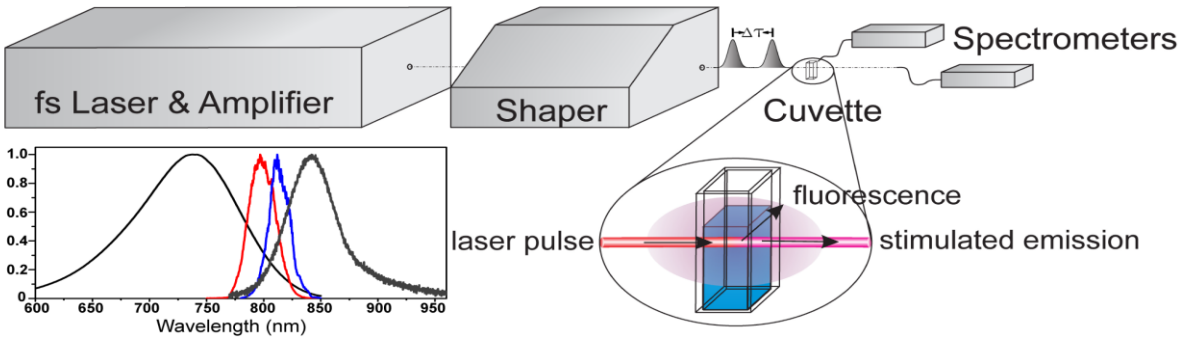

Figure 1. Experimental setup showing the phase and amplitude pulse shaper placed after the amplifier and the simultaneous acquisition of fluorescence and stimulated emission. The absorption (black), laser (red), stimulated emission (blue) and fluorescence (dark gray) spectra for IR 144 are also shown.

~ 700 μJ and was attenuated before entering a phase-amplitude pulse shaper (MIIPS Box 640, Biophotonic Solutions Inc.). The dispersed spectrum covered 450 pixels of the spatial light modulator (SLM) with a resolution of 0.2 nm per pixel. High-order phase distortions introduced by the optics in the laser system and setup are compensated by frequency doubling the laser using a 100 μm thick BBO crystal at the sample plane and running the multiphoton intrapulse interference phase scan (MIIPS) [27, 28] software resulting in 36 fs transform limited pulses at the sample. Phase distortions in the laser pulse have been known to be the source of various artifacts. For example, significant third order dispersion (TOD) introduces sub-pulses with pi-shifted interferometric oscillations (see Figure S1a), therefore it is important to eliminate any such effect in this study. Second harmonic autocorrelations for transform-limited pulses are also provided (Figure S1b). Dispersion from the quartz cell and the path length of the cell when filled with pure methanol was measured and compensated by MIIPS. The dispersion from the input wall is 36 fs^2 and the dispersion of 1 mm of methanol is 30.4 fs^2 [29]. This dispersion if left uncompensated would broaden our 36 fs pulses to 36.4 fs.

Solutions of IR144 and IR125 in methanol (10^{-5} M) were prepared such that they have the same optical density. A 2 mm cuvette was used as the sample holder. The dyes were purchased from Exciton and used without further purification. A collimated, unfocused beam having a diameter (where intensity drops to $1/e^2$) of 4 mm was used to excite the sample. The peak power at the sample was ~10^{10} W/cm^2, leading to 30% excitation probability. The laser was monitored by a first compact spectrometer (not shown) measuring the beam before the cell, fluorescence was monitored by a second compact spectrometer at a right angle from the cell, and the stimulated emission was measured by a third compact spectrometer in the direction of propagation.

B. Phase amplitude shaping

Pairs of identical pulses are generated using a pulse shaper. The design of the phase and amplitude functions is based on a simple but elegant principle of reproducing the complex transfer function of the desired pulses. For example, to mimic a Michelson interferometer the required temporal electric field is

$$E_{out}(t)=\frac{1}{2}\left[E_{in}\left(t-\frac{\tau}{2}\right)+E_{in}\left(t+\frac{\tau}{2}\right)\right] \quad (1)$$

and the corresponding spectral electric field utilizing the Fourier shift theorem is

$$E_{out}(\omega)=\frac{1}{2}\left[\exp\left(-i\omega\frac{\tau}{2}\right)+\exp\left(i\omega\frac{\tau}{2}\right)\right]\cdot E_{in}(\omega)=\cos\left(\omega\frac{\tau}{2}\right)\cdot E_{in}(\omega) \quad (2)$$

The cosine modulation can be implemented by a dual mask phase and amplitude SLM such that $\cos\left(\omega\frac{\tau}{2}\right)=\left|\cos\left(\omega\frac{\tau}{2}\right)\right|\mathrm{sgn}\left[\cos\left(\omega\frac{\tau}{2}\right)\right]$ can be divided into transmission (amplitude squared), $\cos^2\left(\omega\frac{\tau}{2}\right)$ and phase, $\mathrm{sgn}\left[\cos\left(\omega\frac{\tau}{2}\right)\right]$ input modulation. The resulting pair of pulses is identical to the pair that would be created by a Michelson interferometer. However, there are obvious advantages to the pulse shaper. The pulse shaper behaves as a common path interferometer and is capable of introducing extremely small (attosecond) delays with outstanding phase stability, even in the presence of wind currents and vibrations outside the pulse shaper [30, 31].

3. Results and Discussion

Spectral interferometry time-delay scans with transform-limited pulses were performed while simultaneously monitoring the fundamental laser pulses, fluorescence and the coherent stimulated emission for both the dyes as shown in Figure 2. The first pulse is fixed at time zero while the second pulse is scanned interferometrically. All signals are normalized to unity at time zero when the system is being interrogated by a single transform-limited pulse (Figure 2). The early portion of the scan (for $\tau < 80$ fs) shows the expected interferometric modulation caused by the linear optical interference between the laser pulses. Beyond 80 fs the pulses are no longer overlapped and the laser interference oscillations subside (black line, Figure 2). The different asymptotic levels reached at long times fluorescence (red) and stimulated emission (blue) differ from 0.5 because of a slight saturation at zero delay time, as has been discussed previously [13]. Saturation of the ground to excited state transition causes reduced fluorescence and enhanced stimulated emission at zero delay time.

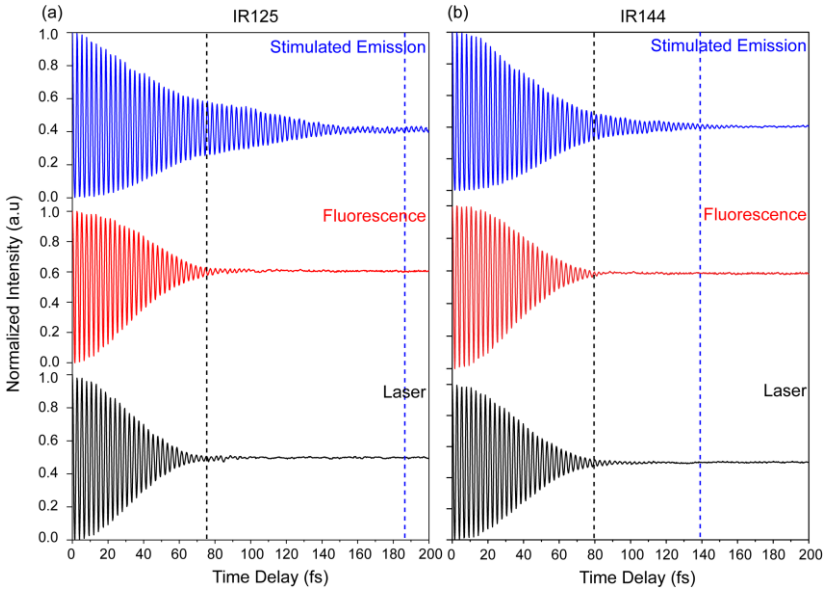

Figure 2. Experimental interferometric time-delay scans for frequency integrated stimulated emission (blue), fluorescence (red), and laser intensity (black) using pair of transform limited pulses generated using phase amplitude modulation. The plots are normalized on excitation with a TL pulse at zero delay time. The vertical lines indicate the time delay when the interferometric oscillations drop to 2% for the excitation pulses (black) and the stimulated emission (blue).

The integrated fluorescence signal (red line, Figure 2) is very similar to the laser integrated intensity (black line, Figure 2); this is not the case for the stimulated emission. Here we explore the optical processes that give rise to the stimulated emission and the observed interferences. We start with an observed quadratic power dependence on laser intensity and linear concentration dependence of the stimulated emission signal (Figure S2). The nonlinear nature of the signal implies it is not simply the Fourier transform of the laser pulse times the excitation spectrum.

Here we consider signals arising from up to three interactions with the laser pulses, i.e. up to third order. The first interaction with an electric field leads to a coherence between ground and excited state $\rho_{eg}^{(1)}$ or $\rho_{ge}^{(1)}$, the second interaction leads to population in the ground or excited states $\rho_{ee}^{(2)}$ or $\rho_{gg}^{(2)}$ and the third interaction leads to a coherence $\rho_{eg}^{(3)}$ or $\rho_{ge}^{(3)}$, responsible for the third-order emission. When excited by two collinear pulses and collecting the stimulated emission, there are a number of possible contributions to the signal. It is possible to rule out signals arising from molecules that only interact with one pulse because such signal would be independent of time delay between the pulses. Similarly, one can ignore the case when two interactions take place with the first pulse because those optical contributions lead to the creation of populations which would not be sensitive to the phase of the second laser pulse.

Phase-sensitive interference implies the signal arises from (a) cases when molecules interact once with the first pulse and twice more with the second pulse, or (b) cases when the molecules interact three times with one pulse and the third-order polarization from such an interaction is heterodyned by the other pulse. Cases (a) give rise to both rephasing (photon echo) and non-rephasing signals; however the non-rephasing signal decays exponentially from the time of the first pulse. The rephasing signal is more intense, has a Gaussian type of decay, and dominates at longer times. For cases (b), because all three interactions occur with one of the pulses, there is no difference between non-rephasing and rephasing signals.

The inhomogeneously broadened Stokes shifted electronic excited state causes the emission to be red shifted. In both cases (a) and (b) there is a third order signal with the emitted field $E_{Sig}^{(3)}(t)$ and the detected signal is heterodyned by the present laser field $E_l(t)$ according to $I_{Sig} \propto \mathrm{Re}\int_0^\infty \left\{E_l(t)E_{Sig}^{(3)}(t)\right\}dt \propto E_l E_l^3 \propto I_l^2$. Notice the signal intensity is proportional to the intensity of the laser (both pulses integrated) squared, i.e. proportional to I_l^2. The resulting field in the time domain is Fourier transformed by the spectrometer to produce an emission spectrum for each time delay. We plot the total integrated signal corresponding to each spectral component to produce the oscillatory trace (blue lines) in Figure 2. The long lived nature of the oscillations can be attributed to the $\rho_{eg}^{(3)}$ matrix element that is generated after the third interaction with the laser pulse. The signal is initially masked by the linear optical interference but the out of phase nature of the oscillations is gradually revealed once the optical interference of the laser fields subsides, after ~80 fs in Figure 2.

Phenomenological fitting based on reconstruction of the different signal sources is possible. During an interferometric scan the total energy of the pulse pair depends on the time delay due to linear optical interference. In the case of a Gaussian laser spectrum the formula that describes this dependence is $\frac{1}{2}+\frac{1}{2}\exp\left[-\left(0.5\frac{\tau}{\tau_0}\right)^2\right]\cos(\omega_0 t)$, where τ is the delay time, ω_0 the carrier frequency and τ_0 the pulse duration. In order to interpret the experimental data, we start with nonlinear fitting using Eq. 3 to simulate changes in the intensity of the laser field by itself as a function of time delay.

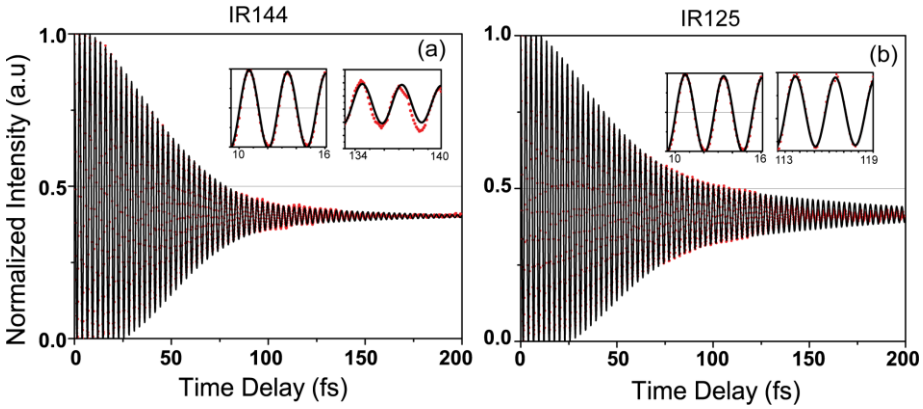

Figure 3. Experimental data (red dots) and the best fit curve (black line) for stimulated emission generated by the pair of the delayed pulses for (a) IR144 and (b) IR125. The inset shows the fit quality for both the datasets at early and later times.

$$I(\tau) = a + \alpha \exp\left[-\left(0.5\frac{\tau}{\tau_0}\right)^2\right]\cos(\omega_0\tau) \quad (3)$$

Fitting of the experimental fundamental laser data results in the parameters a = 0.503, α = 0.507, ω_0 = 2.355 fs^{-1} and τ_0 = 21.5 fs which are very close to the expected values (the value of τ_0 corresponds to 35.8 fs FWHM). The expected values are 0.5, 0.5, 2.356 fs^{-1} and 21.5 fs respectively, where the carrier frequency and duration of TL pulse were calculated using Gaussian fitting of the pulse spectrum. Comparison of the experimental laser intensity and the fitted curve is shown in Figure S3a.

The dependence of fluorescence with respect to the time delay between pulses is a bit more complicated compared to the energy of the pulse, because of the nonlinear optical process of fluorescence saturation (Figure S3b). At the highest laser intensity, the fluorescence is smaller than predicted by linear absorption. The saturation effect can be phenomenologically included. Eq. 4 and 5 simulate the dependence of fluorescence as a function of time delay.

$$F(\tau) = F_m(\tau) + \exp\left[-\left(0.5\frac{\tau}{\tau_0}\right)^2\right]\cos(\omega_0\tau) \quad (4)$$

$$F_m(\tau) = a_m + (0.5 - a_m)\exp\left(-\frac{\tau^2}{\tau_f^2}\right) \quad (5)$$

Fluorescence saturation is taken into account by introducing a decrease of the mean value of the curve $F_m(\tau)$ with a rate comparable to the pulse duration. The best parameters that fit the experimental data are a_m = 0.58, ω_0 = 2.361 fs^{-1}, τ_f = 22 fs. Here τ_f corresponds to 36.6 fs FWHM and the expected pulse duration taking dispersion into account is 36.4 fs.

The stimulated emission signal for both dyes, in addition to showing nonlinear amplification at higher power clearly shows an additional long-lived modulation as shown in Figure 3a and b. These two effects can also be included in the phenomenological equations to fit the experimental data. These three effects are included in the phenomenological Eq. 6-8 for fitting of the stimulated emission signal.

$$S(\tau) = S_{sat}(\tau) + 0.5\exp\left[-\left(0.5\frac{\tau}{\tau_0}\right)^2\right]\cos(\omega_d\tau) + S_{tail}(\tau) \quad (6)$$

$$S_{sat}(\tau) = a_{sat} + (0.5 - a_{sat})\exp\left(-\frac{\tau^2}{\tau_0^2}\right) \quad (7)$$

$$S_{tail}(\tau) = a_{tail}\cos(\omega_{tail}\tau + 0.5\pi)\exp\left(-\frac{\tau^2}{\tau_{tail}^2}\right) \quad (8)$$

The best parameters that fit the experimental data for IR144 are: a_{sat} = 0.4, a_{tail} = 0.1, ω_{tail} = 2.314 fs^{-1}, ω_d = 2.34 fs^{-1}, τ_0 = 23 fs, τ_{tail} = 110 fs. In this case τ_0 = 23 fs corresponds to 38 fs FWHM. The fit quality is demonstrated by showing the zoomed in regions from the early and later times (Figure 3c and d inset). A point worth noting is that in spite of the simulation introducing a $\pi/2$ shift in the long-lived oscillations, we ultimately see a gradual π shift at long times beyond 140 fs for both the dyes. The extracted parameters for IR125 are ω_{tail} = 2.308 fs^{-1}, ω_d = 2.32 fs^{-1}, τ_0 = 23 fs, τ_{tail} = 170 fs. The reason for the decrease in observed oscillation frequency for the long-lived tail ω_z = 2.314 fs^{-1} for IR144 and 2.308 fs^{-1} for IR125 compared to the ω_0 = 2.355 fs^{-1} can be correlated to the emission from a lower energy Stokes shifted state upon solvation. The main difference between both dyes is the relatively floppy piperazine-ethyl ester nitrogen attached to the conjugated chain in IR144 [23] (Figure S5).

Analysis of the stimulated emission fit for IR144 shown in Figure 4 allows us to observe the enhancement of the signal at early times, which leads to a lower asymptotic value. The out-of-phase oscillations, which can be easily isolated from the phenomenological model, are plotted in Figure 4. They are found to follow Gaussian type of decay instead of an exponential one which may be caused by the rephasing nature of the observed signal. The gradual change in phase is clearly seen in the extracted phase (Figure S4). The observed stimulated emission interferences are not caused by any phase distortion in the pulses. The reader is referred to the experimental second harmonic autocorrelations of the transform limited pulses and also how high-order dispersion causes different interference features with characteristic π steps (See Figure S1).

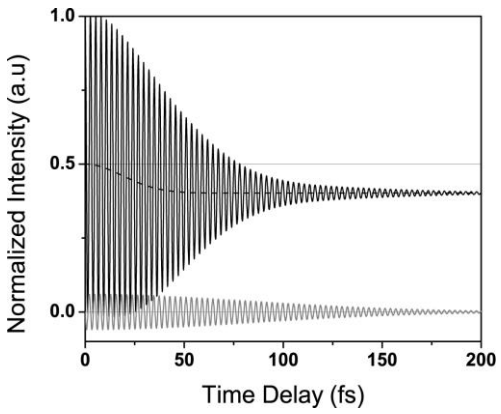

Figure 4. Simulation of the stimulated emission signal for IR144 in methanol (solid black line), mean value of fast component (black dash) and long lived delayed component (gray line) showing $\pi/2$ shifted oscillations.

4. Conclusions

The femtosecond nonlinear optical response and dephasing rate of laser dyes IR144 and IR125 in solution is explored, taking advantage of high-resolution pulse synthesis using a pulse shaper. Fluorescence and stimulated emission interferograms were obtained with attosecond resolution. We found that the stimulated emission shows interferometric modulation that is shifted out of phase from the early time modulation as opposed to fluorescence which was short lived and not phase shifted. The long-lived out-of-phase stimulated emission oscillations are assigned to a rephasing third-order signal reflecting the coherence between the Stokes-shifted excited state and the ground state.

In conclusion, the ability to manipulate the phase and amplitude of femtosecond pulses provides a simple yet powerful tool to re-visit some of the key aspects of molecular spectroscopy such as absorption, fluorescence and stimulated emission. Our measurements allow us to follow and compare the electronic dephasing rate for two closely related molecules. Our finding is that dephasing rates for these molecules are of the order of 130 fs and 180fs for IR144 or IR125, respectively. The single-shaped laser pulse approach followed here to make these measurements may be compatible with single-molecule measurements being contemplated.

Acknowledgements

We thank DOE SISGR (DE-SC0002325), Dr. Jeff Krause, Program Manager for support of this research. MD gratefully acknowledges discussions with Profs. Shaul Mukamel, Graham Fleming and Ahmed Zewail about these results.

References

1. T. Brixner, J. Stenger, H. M. Vaswani, M. Cho, R. E. Blankenship, and G. R. Fleming, Nature 434 (2005) 625.
2. Y. C. Cheng, and R. J. Silbey, Phys. Rev. Lett. 96 (2006) 028103.
3. A. Ishizaki, T. R. Calhoun, G. S. Schlau-Cohen, and G. R. Fleming, PCCP 12 (2010) 7319.
4. V. Wong, and M. Gruebele, Phys. Rev. A. 63 (2001) 022502.
5. G. S. Engel, T. R. Calhoun, E. L. Read, T. K. Ahn, T. Mancal, Y. C. Cheng, R. E. Blankenship, and G. R. Fleming, Nature 446 (2007) 782.
6. Y. C. Cheng, and G. R. Fleming, Annu. Rev. Phys. Chem. 60 (2009) 241.
7. N. Dudovich, D. Oron, and Y. Silberberg, Nature 418 (2002) 512.
8. D. Oron, N. Dudovich, D. Yelin, and Y. Silberberg, Phys. Rev. Lett. 88 (2002) 063004.
9. P. Tian, D. Keusters, Y. Suzaki, and W. S. Warren, Science 300 (2003) 1553.
10. C. Li, W. Wagner, M. Ciocca, and W. S. Warren, J. Chem. Phys. 126 (2007) 164307.
11. M. T. Bremer, P. J. Wrzesinski, N. Butcher, V. V. Lozovoy, and M. Dantus, Appl. Phys. Lett. 99 (2011) 101109.
12. A. Konar, V. V. Lozovoy, and M. Dantus, J. Phys. Chem. Lett. 3 (2012) 2458.
13. A. Konar, J. D. Shah, V. V. Lozovoy, and M. Dantus, J. Phys. Chem. Lett. 3 (2012) 1329.
14. A. Konar, V. V. Lozovoy and M. Dantus, J. Phys. Chem. Lett. 5 (2014) 924.
15. S. Y. Lee, and E. J. Heller, J. Chem. Phys. 71 (1979) 4777.
16. V. Blanchet, M. A. Bouchène, and B. Girard, J. Chem. Phys. 108 (1998) 4862.
17. E. J. Heller, In: C. Harris, E. Ippen, G. Mourou and A. Zewail (Eds.), Ultrafast Phenomena VII, Springer, Berlin Vol. 53 (1990) pp. 418-422.
18. R. R. Jones, C. S. Raman, D. W. Schumacher, and P. H. Bucksbaum, Phys. Rev. Lett. 71 (1993) 2575.
19. R. R. Jones, Phys. Rev. Lett. 75 (1995) 1491.
20. R. R. Jones, D. W. Schumacher, T. F. Gallagher, and P. H. Bucksbaum, J. Phys. B 28 (1995) L-405.
21. W. Wagner, C. Q. Li, J. Semmlow, and W. S. Warren, Opt. Express 13 (2005) 3697.
22. G. A. Lott, A. Perdomo-Ortiz, J. K. Utterback, J. R. Widom, A. Aspuru-Guzik, and A. H. Marcus, PNAS 108 (2011) 16521.
23. A. C. Yu, C. A. Tolbert, D. A. Farrow, and D. M. Jonas, J. Phys. Chem. A 106 (2002) 9407.
24. J. D. Hybl, S. M. G. Faeder, A. W. Albrecht, C. A. Tolbert, D. C. Green, and D. M. Jonas, J. Lumin. 87-89 (2000) 126.
25. E. A. Carson, W. M. Diffey, K. R. Shelly, S. Lampa-Pastirk, K. L. Dillman, J. M. Schleicher, and W. F. Beck, J. Phys. Chem. A 108 (2004) 1489.
26. S. Park, J. S. Park, and T. Joo, J. Phys. Chem. A 115 (2011) 3973.
27. Y. Coello, V. V. Lozovoy, T. C. Gunaratne, B. W. Xu, I. Borukhovich, C. H. Tseng, T. Weinacht, and M. Dantus, J. Opt. Soc. Am. B 25 (2008) A140.
28. V. V. Lozovoy, I. Pastirk, K. A. Walowicz, and M. Dantus, J. Chem. Phys. 118 (2003) 3187.
29. P. Devi, V. V. Lozovoy, and M. Dantus, AIP Adv. 1 (2011) 032166.
30. A. M. Weiner, Rev. Sci. Instrum. 71 (2000) 1929.
31. A. Präkelt, M. Wollenhaupt, C. Sarpe-Tudoran, and T. Baumert, Phys. Rev. A 70 (2004) 063407.

Cite this article as:

Arkaprabha Konar *et al.*: **Electronic dephasing of molecules in solution measured by nonlinear spectral inteferometry.** ScienceJet 2015, **4**: 141